

Electronic Supplementary Information

Supramolecular chirality induced by a weak thermal force†

Placido Mineo,*^{a,b} Valentina Villari,*^b Emilio Scamporrino^a and Norberto Micali^b

^a *Dipartimento di Scienze Chimiche and I.N.S.T.M. UdR of Catania, University of Catania, Viale Andrea Doria 6, I-95125 Catania, Italy. E-mail: gmineo@unict.it*

^b *CNR-IPCF Istituto per i Processi Chimico-Fisici, Viale F. Stagno d'Alcontres 37, Messina, Italy. E-mail: villari@me.cnr.it*

Content

1) Materials and Methods:

- Materials.
- MALDI-TOF spectrum of PPeg4. Figure S1
- ¹H-NMR spectrum of PPeg4. Figure S2
- Experimental details. Figure S3: Top-view of the Jasco PTC-423S/15 Peltier-type temperature control system. Figure S4: Scheme of the home-made thermostat and induced temperature gradient.

2) Spontaneously self-assembled structures in water:

- Size distribution of PPeg4 aggregates at 26°C: Figure S5
- Fitting equation for static light scattering profile: Equation 1.

3) CD band features dependence on the experimental procedure according to which a temperature value is reached:

- Spectroscopic features of PPeg4 solution during heating with the standard Jasco thermostat: Figure S6
- Spectroscopic features of PPeg4 solution during cooling with the standard Jasco thermostat: Figure S7

4) Light scattered intensity profile at different temperature values:

- Figure S8

5) Evaluation of the contribution of LD into the CD spectra:

- Scheme of the apparatus built-up to measure linear dichroism and cuvette birefringence:

Figure S9

- Equations describing CD and LD signals: Equations 2 and 3

- Linear (LD) and circular (CD) dichroism spectra as a function of the rotation angle θ for the thermostated sample in the presence of temperature gradient (through the single-stage home-made thermostat): Figure S10

-Linear (LD) and circular (CD) dichroism spectra as a function of the rotation angle θ for the thermostated sample in the absence of temperature gradient (through the two-stage home-made thermostat): Figure S11

1) Materials and Methods:

Materials. All the solvents and basic materials were commercial products (Sigma-Aldrich) properly purified before use. The molecule 5,10,15,20-tetrakis[p(ω -methoxy-polyethyleneoxy)phenyl]porphyrin (PPeg4) was obtained by synthesis;^[1-3] its MALDI-TOF and ¹H-NMR spectra are reported in Figure S1 and S2, respectively.

The PPeg4 concentration was 4 μ M both in Tetrahydrofuran (THF) and water. For the absorption measurement a cuvette with 0.5 cm optical path was used for THF and with 1 cm optical path for water. The value of concentration has been chosen as a compromise between a good spectroscopic signal (related to the aggregates size, which, for analogous molecules was shown to increase with increasing concentration^[4]) and a proper absorption value.

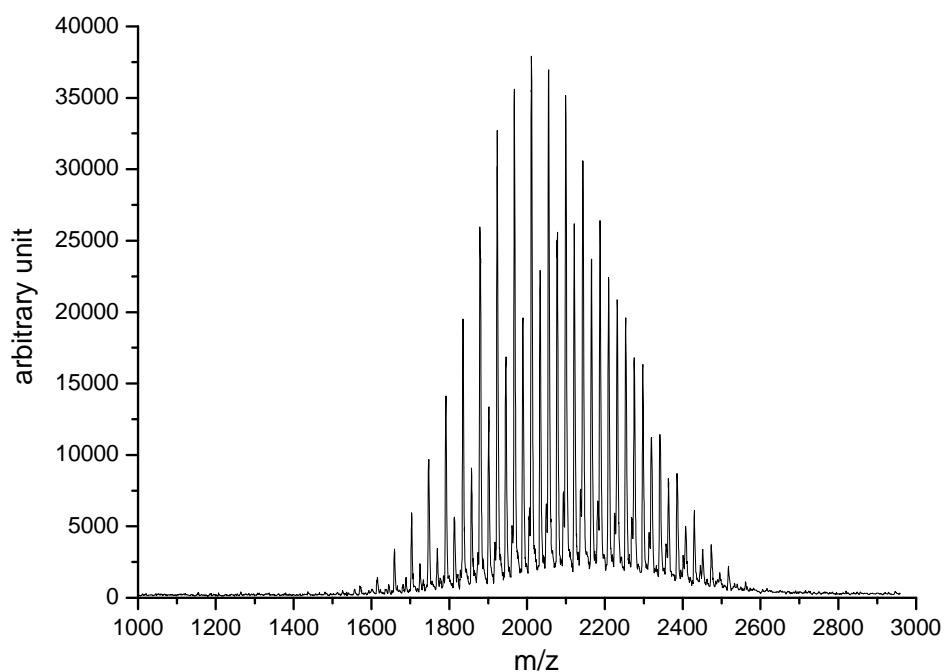


Figure S1: MALDI-TOF spectrum of PPeg4. The mass spectrum is constituted of two series of peaks at m/z values of $735+n44$ (with $n= 19-40$, first peak in the spectrum at m/z 1571) and $757+n44$ (with $n=20-41$, first peak in the spectrum at m/z 1637), corresponding to oligomers cationized with H^+ or Na^+ , respectively.

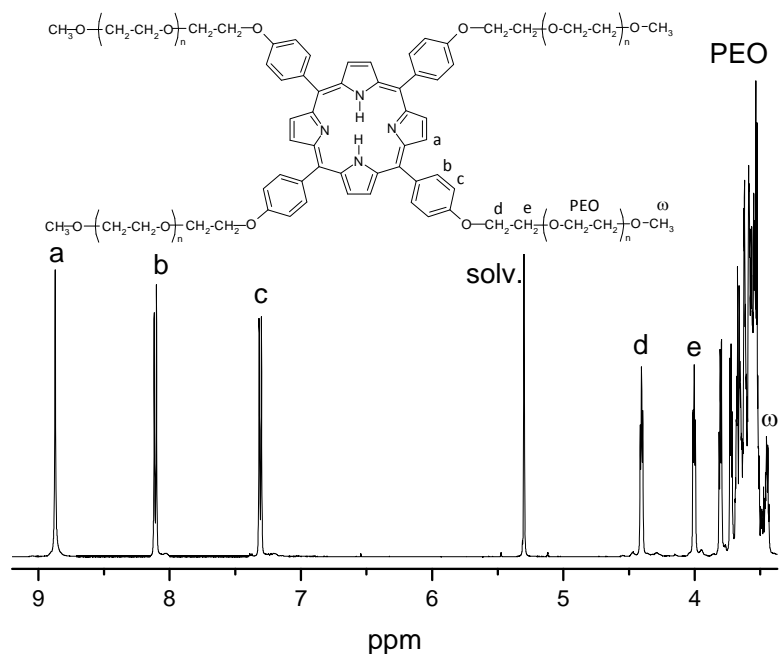


Figure S2: $^1\text{H-NMR}$ spectrum of PPeg4. $^1\text{H-NMR}$ assignment (500 MHz, CD_2Cl_2 , ppm): a singlet at 8.90 (8 H, C-H pyrrole protons, *a*), two doublets at 8.13 ($J=8.6$ Hz; 8 H, C-H phenyl protons, *b*) and at 7.32 ppm ($J=8.6$ Hz; 8 H, C-H phenyl protons, *c*), a singlet at -2.803 ppm (2 H, N-H pyrrole protons); signals due to the PEG arms: two triplets centered at 4.42 and 4.02 ppm (for a total of 16 H, CH_2 groups, *d* and *e*), an unresolved multiplet between 3.85 and 3.43 ppm (about 128 H, the other methylene groups of the polyethylene oxide, PEO), few singlet between 3.33 and 3.30 ppm (12 H, the $-\text{OCH}_3$ terminal groups of the branches, ω).

Experimental details

The chemical structure of the synthesized compounds was characterized by $^1\text{H-NMR}$ and MALDI-TOF analyses. $^1\text{H-NMR}$ spectra were obtained on a UNITY^{INNOVA} Varian instrument operating at 500 MHz using VNMR for software acquisition and processing. Samples were dissolved in CD_2Cl_2 and the chemical shifts were expressed in ppm compared to the CH_2Cl_2 residue signal. The spectra were acquired at 300 K, with a spin lock time of 0,5 s. Positive MALDI-TOF mass spectra were acquired by a Voyager DE-STR (PerSeptive Biosystem) using a simultaneous delay extraction procedure (25 kV applied after 2600 ns with a potential gradient of 454 V/mm and a wire voltage of 25 V) and detection in linear mode. The instrument was equipped with a nitrogen laser (emission at 337 nm for 3 ns) and a

flash AD converter (time base 2 ns). Trans-3-indoleacrylic acid (IAA) was used as a matrix. Mass spectrometer calibration was performed as reported in previous cases.^[1,5] The m/z values reported in the spectra and in text refer to molecular ions of the most abundant isotope of each element in the molecule.

UV-visible spectra were recorded at $T=25^{\circ}\text{C}$ by a Shimadzu Model 1601 spectrophotometer, in quartz cells, using Tetrahydrofurane or Water as a solvent.

The circular dichroism spectra were recorded by means of two different JASCO instruments: J-815 and J-500A spectropolarimeters, both equipped with a 150W Xenon lamp. The ellipticity, $\theta \propto \varepsilon_L - \varepsilon_R$, was obtained calibrating the instruments with a 0.06 percent (w/v) aqueous solution of ammonium d-10-camphorsulfonate and with a 0.08 percent (w/v) aqueous solution of Tris (ethylendiamine) Co complex ($2(-)\text{D}[\text{Coen}_3]\text{Cl}_3 \cdot \text{NaCl} \cdot 6\text{H}_2\text{O}$). The measurements, corrected for the contribution from cell and solvent, were performed at constant or at variable temperature in quartz cells, using water as a solvent. The temperature of J-815 was controlled by means of a Jasco PTC-423S/15 Peltier-type temperature control system (cooled with an external water circulator, see Figure S3).

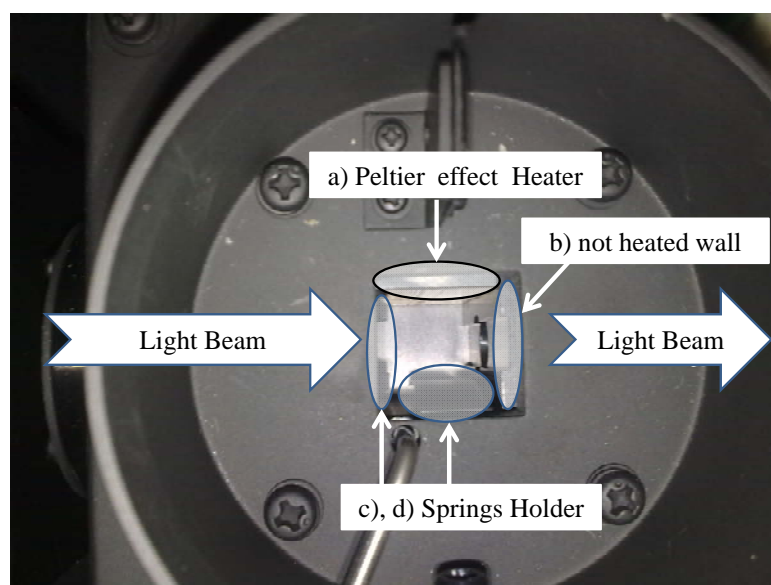


Figure S3: Top-view of the Jasco PTC-423S/15 Peltier-type temperature control system. The first wall (a) is at contact with the heater; the second wall (b) is at contact with (a), but it is not directly heated; the other two are in contact with springs that hold the cuvette into the thermostating holder (c and d).

The temperature of J-500A (with home-made modifications) was controlled by means of a home-made thermostat consisting of an insulated copper block (with water-circulating wires in the interior controlled by a HAAKE F6-C25 thermostat) with 12.7 millimetre-sized squared hole for inserting the cuvette (having 1 cm path length) and 5 millimetre-sized apertures for the beam passing through the sample.

Such a thermostating apparatus avoided convections and the generated vortex arose from the thermophoresis from the hotter to the colder zones, as the combination between a circular and a vertical flow along the temperature gradients (see Figure S4).

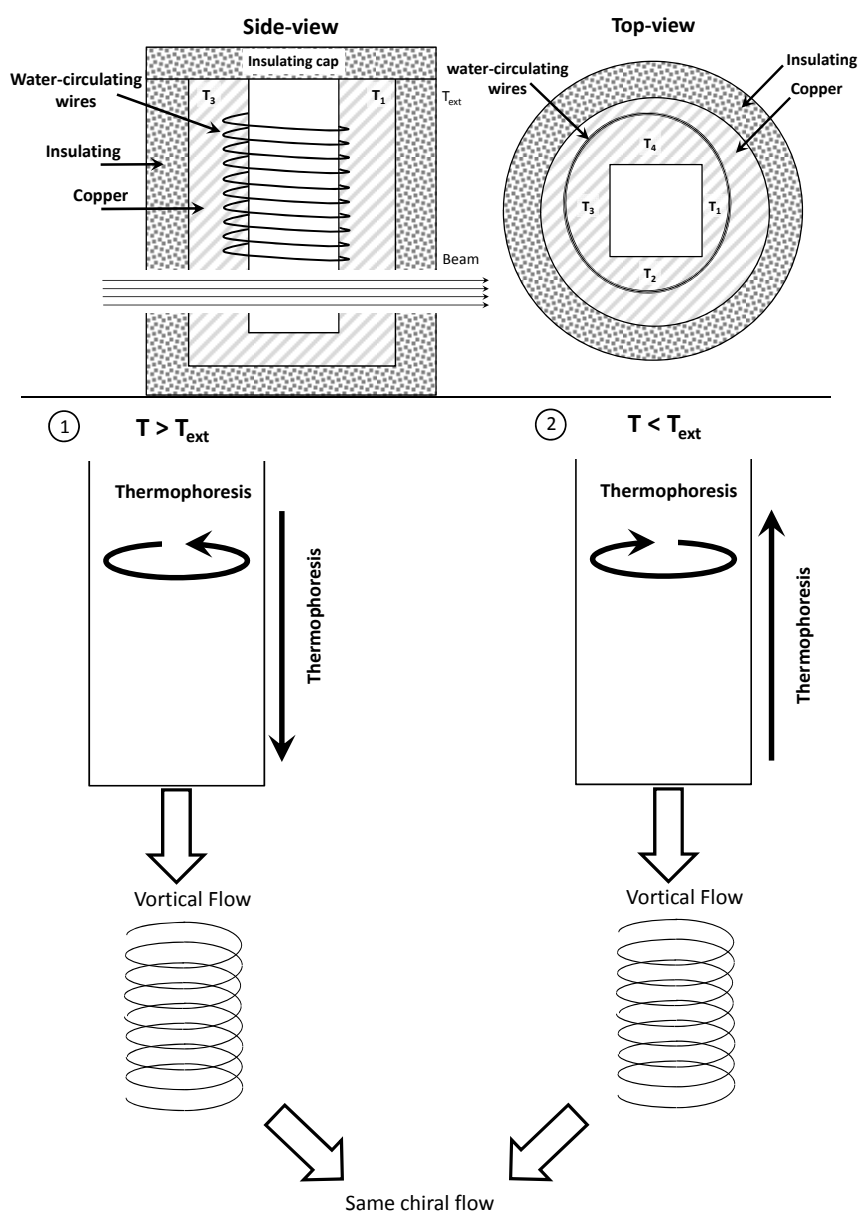


Figure S4: Scheme of the home-made thermostat and induced temperature gradient. Two temperature gradients are generated by the home-made thermostat and thermophoresis from the hotter to the colder zones occurs. A circular thermophoretic motion due to the different temperature of the cuvette's walls and vertical one due to the difference in the temperature between top and bottom of the cuvette: the resulting effect is a vortical flow. In particular, when $T > T_{\text{ext}}$ temperatures T_1 and T_2 (with $T_1 > T_2$) of the cuvette walls are higher than T_3 and T_4 ; in addition, the temperature of the bottom of the cuvette is lower than its upper part. Because both the gradients (and hence thermophoresis) invert when temperature is set below the external one, $T < T_{\text{ext}}$, the resulting vortical flow remains the same.

In order to improve further the temperature stability, so eliminating temperature gradients, a two-stage thermostating process was adopted, by inserting the thermostat in a box. The air in the box was thermostated at the same temperature as the sample.

Static light scattering (ELS) and Dynamic Light Scattering (QELS) experiments have been performed at small and wide angles using an He-Ne laser and an homemade apparatus already described in the literature.^[6]

UV-vis, circular dichroism and light scattering measurements were performed at a concentration of 4×10^{-6} M.

Particular care was devoted to the choice of the cuvette (4 windows Hellma cell) with low birefringence (see section 6).

2) Spontaneously self-assembled structures in water:

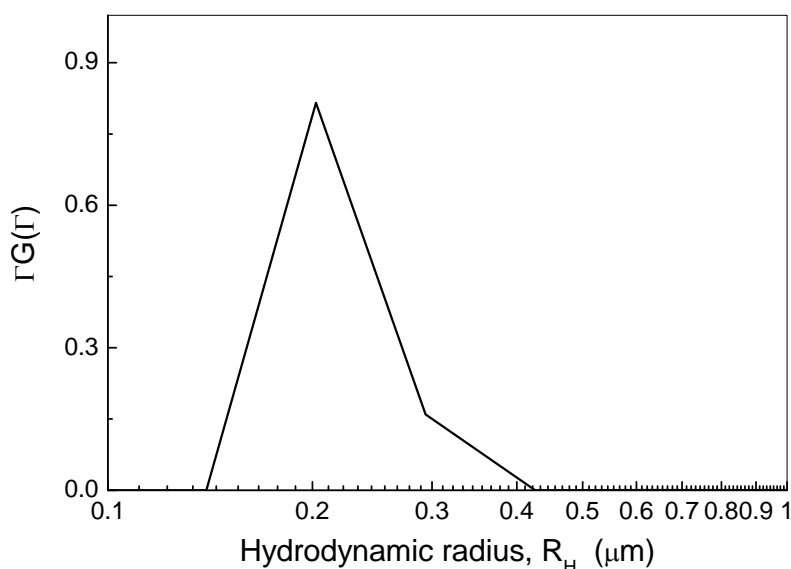


Figure S5: Size distribution of PPEG4 aggregates at 26°C. The size distribution was obtained by performing the inversion (using the algorithm CONTIN) of the dynamic light scattering data^[3]. Size distribution, measured at different temperature values, does not show any change.

Fitting equation for static light scattering profile: Equation 1

$$I(Q) \propto \frac{\sin[(D_f - 1)\arctan(QR)]}{(D_f - 1)QR(1 + Q^2R^2)^{(D_f - 1)/2}} \quad (1)$$

In order to fit the scattered intensity profile obtained by static light scattering we used, in the whole Q range investigated, a fit law for finite fractal systems deduced by Chen and Teixeira.^[7] In this equation R is the radius of the aggregate, namely the cut-off parameter of the density correlation function of the fractal, and D_f is the fractal dimension. The latter measures the scaling law between the mass and the size of the aggregate. From the fit parameters the radius of gyration is calculated through

$$R_g = \left(\frac{D_f}{2 + D_f} R^2 \right)^{\frac{1}{2}}. [3]$$

3) CD band features dependence on the experimental procedure according to which a temperature value is reached:

The CD band features (sign, shape and strength) are strongly dependent on the experimental procedure according to which a temperature value is reached. As an example, in Figures S4 and S5 two series of spectra were recorded, respectively, on increasing temperatures from 26 to 36 °C and successively on decreasing temperature from 36 to 26 °C. During the heating process from 26°C (and the cooling process from 36°C), the CD bands change sign and, gradually, their intensity increases (decreases); also in this case, to all the changes in the CD spectra, no change corresponds in the absorption profiles.

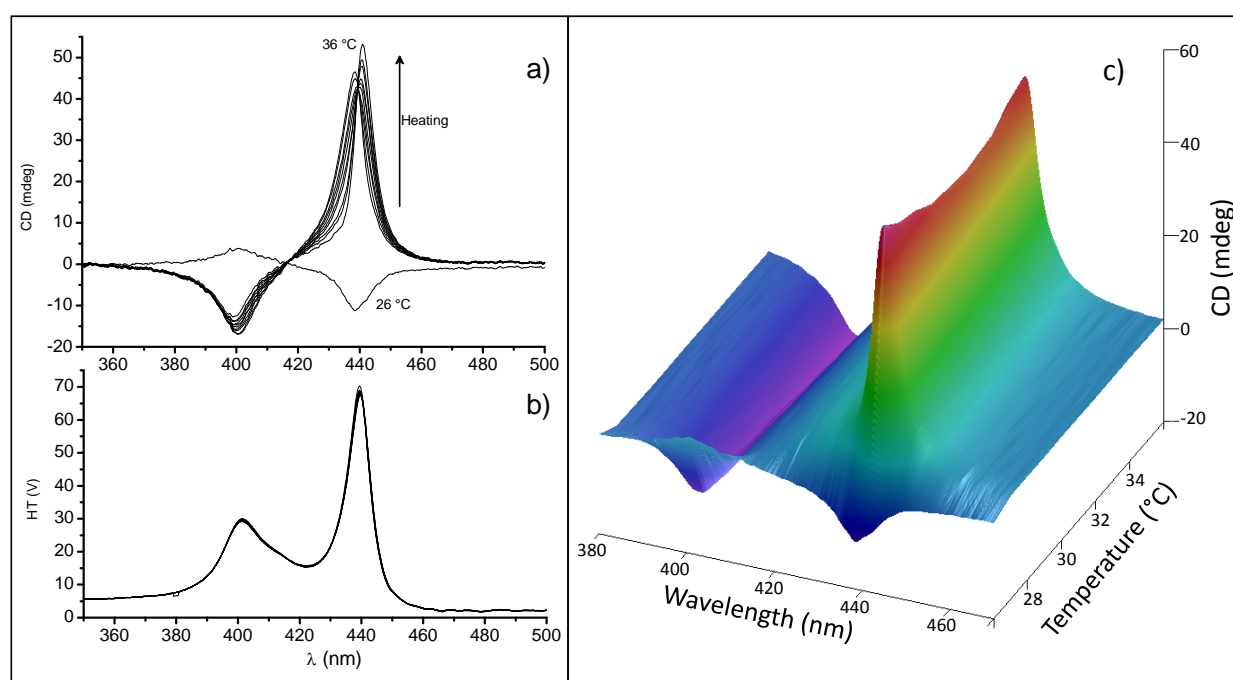


Figure S6: Spectroscopic features of PPEG4 solution during heating: a) Circular Dichroism spectroscopy experiments upon heating (from 26 to 36 °C, 1 °C/min) of PPEG4 solution, performed by means of the JASCO Peltier-type thermostat. The first scan at 26 °C (hold at 26 °C for 210 minutes before the temperature scanning) shows weak signals, at 400 nm (+4 mdeg) and 440 nm (-11 mdeg). The heating process determines a change of the CD sign and an increase of CD strength. b) The absorption spectrum (measured by the high tension, HT, of the detector) remains, instead, unchanged upon heating; c) 3D visualization of the CD spectra during heating.

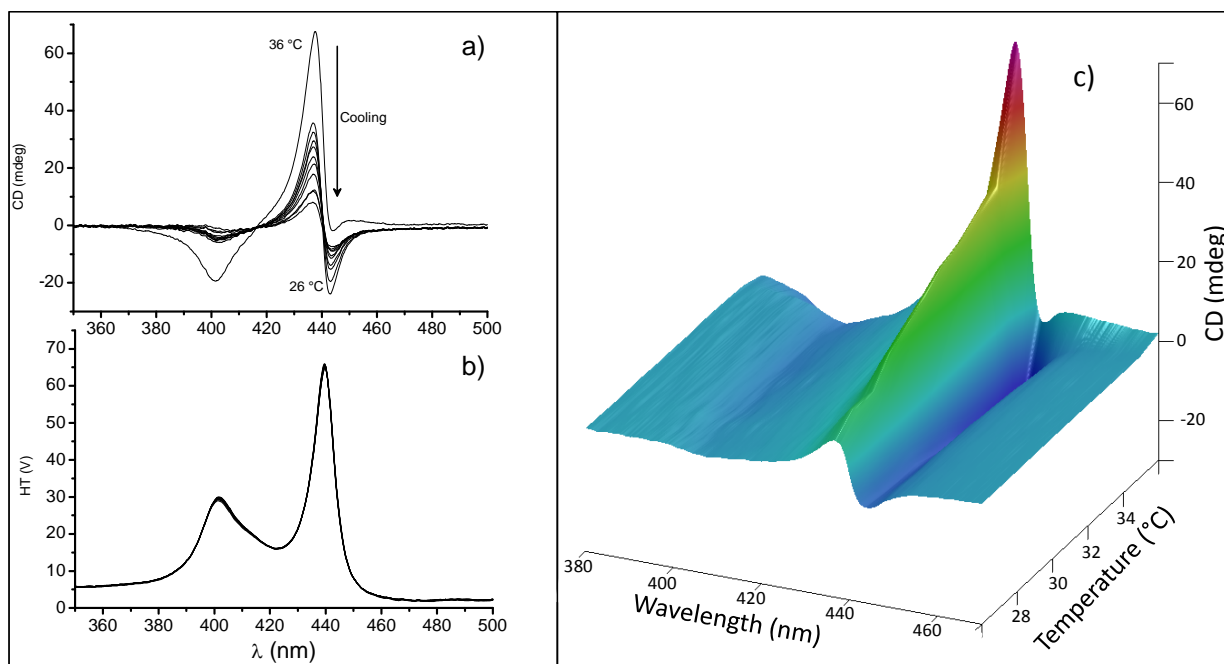


Figure S7: Spectroscopic features of PPEG4 solution during cooling: a) Circular Dichroism spectroscopy experiments upon cooling (from 36 to 26 °C, -1 °C/min) of PPEG4 solution, performed by means of the JASCO Peltier-type thermostat. The starting spectrum (at 36 °C, collected after 240 min.) has a negative band (-19 mdeg) at 400 nm and an asymmetric band at about 440 nm (+68 mdeg). At the end of the run (26 °C) a change of the sign of the band at 400 nm (up to about +1 mdeg) is evident, whereas the band centered at 440 nm becomes almost symmetric (-7 mdeg, +9 mdeg.). b) To all these changes, no change appears in the absorption spectrum upon cooling. c) 3D visualization of the CD spectra during cooling.

4) Light scattered intensity profile at different temperature values.

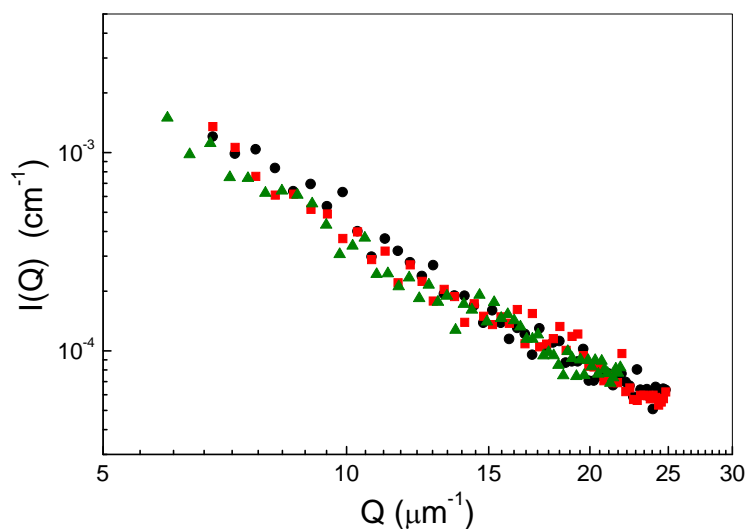
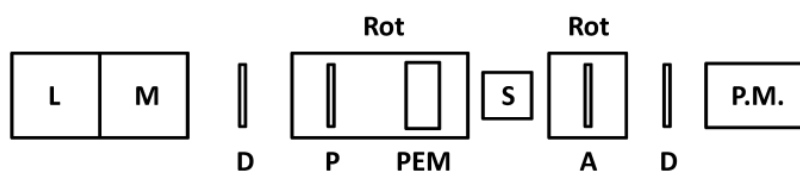


Figure S8: The mesoscopic structure of the PPEG4 aggregates in water does not depend on the temperature of sample; the scattered intensity profile, in fact, remains unchanged in the same temperature range as in the circular dichroism experiments (T=26°C, circles; T=30°C, squares; T=36°C, up triangles).

5) Evaluation of the contribution of LD into the CD spectra:



- L= Lamp
- M= Monochromator
- D= Depolarizer
- P= Polarizer
- PEM= Photoelastic modulator
- ROT= Rotator
- S= Sample
- A= Analyzer
- P.M.= Photomultiplier

Figure S9: Scheme of the apparatus built-up to measure linear dichroism and cuvette birefringence. The measurements of linear (LD) and circular dichroism (CD) were carried out at different rotation angle, θ , of the polarizator/PE modulator system, defined as relative to the horizontal orientation. The analyzer A was used for the calibration of LD and for the separate measurement of the birefringence of the cuvette. All these measurements allowed for evaluating quantitatively the cross-talk between LD and CD.

Equations 2 and 3 describing CD and LD signals and determination of cuvette's birefringence.

Because of the small residual static birefringence of the PE modulator and of the geometry of detection (depolarizator/photomultiplier system), the equations for the measured signals for circular and linear dichroism can be written as:

$$CD_{app} = G1[CD + 0.5(LD'LB - LDLB') + (LD' \sin 2\theta - LD \cos 2\theta) \sin \alpha] \quad (2)$$

$$LD_{app} = G2 (LD' \sin 2\theta - LD \cos 2\theta) = LD \quad (3)$$

where G1 and G2 are known from calibration.

Here LB and LD are the linear birefringence (with magnitude LB_{β}) and the linear dichroism (with magnitude LD_{χ}), respectively. LD' is the 45° linear dichroism, θ the rotation angle of the sample with respect to the polarizator/PE modulator system and α the residual static birefringence of PE modulator. CD_{app} changes with θ only through the last term, which is negligible for small residual stress of the PE modulator and/or for small value of linear dichroism.

From the measurement of the birefringence of the optical system (performed with water-containing cuvette) we found that LB magnitude was 0.012 with orientation of $\beta \cong 52^\circ$ (with respect to the horizontal orientation set as zero angle) at 440 nm. In the wavelength range of interest LB variations occur only within some percent.

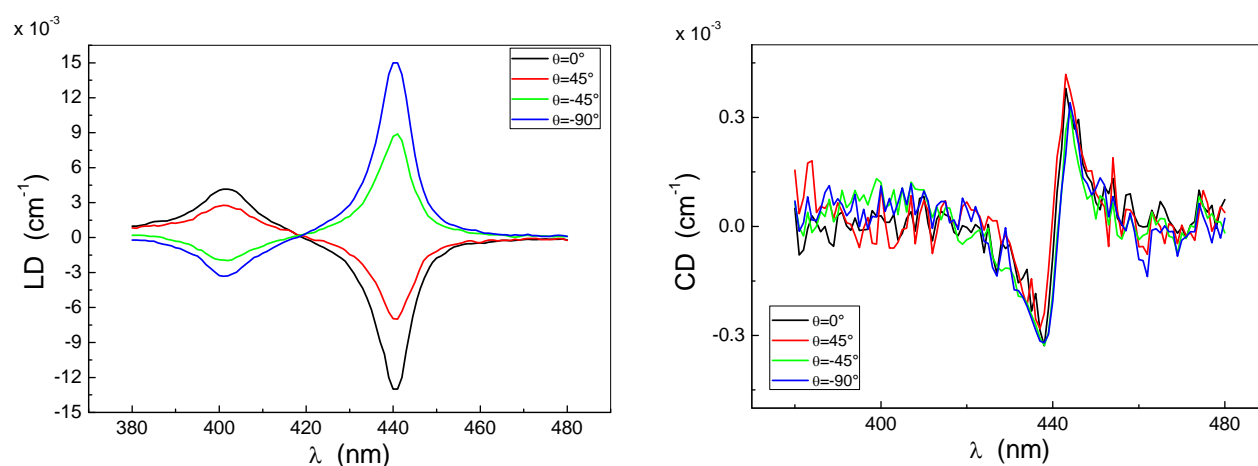


Figure S10: Linear (LD) and circular (CD) dichroism spectra as a function of the rotation angle θ for the thermostated sample in the presence of temperature gradient (through the single-stage home-made thermostat). From the LD magnitude ($LD_{\chi} = 0.015 \text{ cm}^{-1}$) at the wavelength of the absorption maximum (440nm), obtained by the equation 2 describing LD signal, from the CD strength (0.0007 cm^{-1}) and from the linear birefringence of the cuvette ($LB \approx 0.012$), it was calculated^[8,9] that the contribution of LD in the CD spectrum (i.e. the contribution of the second term of CD_{app} equation) is less than 5%. The unchanged CD spectra under θ variations indicates that the third term of CD_{app} (originated from the residual static birefringence of PE modulator α) can be neglected. The sample temperature was set at 36°C and the room temperature at 22°C. For sake of comparison both LD and CD are reported in cm^{-1} units.

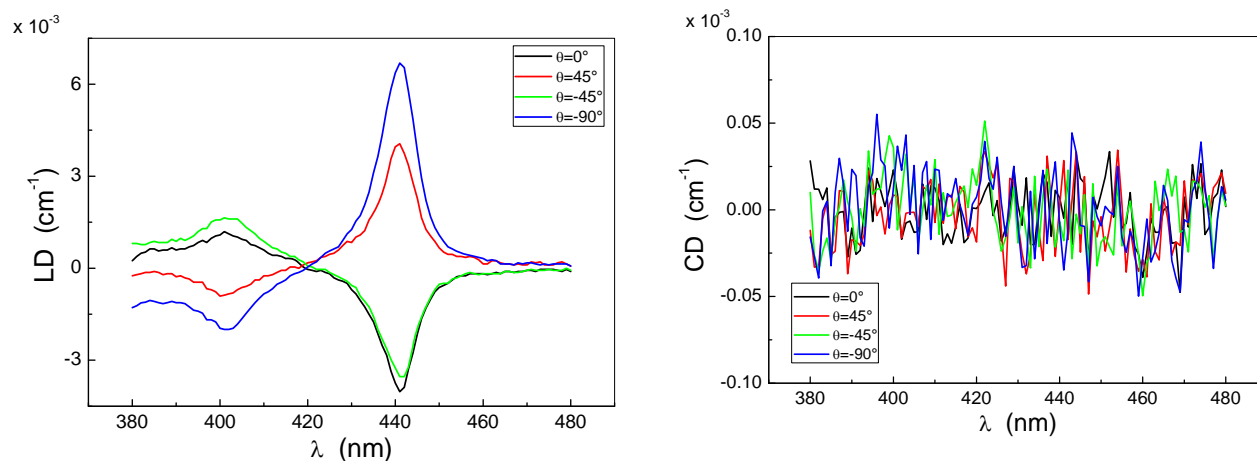


Figure S11: Linear (LD) and circular (CD) dichroism spectra as a function of the rotation angle θ for the thermostated sample in the absence of temperature gradient. The measurements of both LD and CD, by using the two-stage home-made thermostat, put in evidence that there is no contribution from LD into CD spectra. For sake of comparison both LD and CD are reported in cm^{-1} units.

References

- 1 E. Scamporrino, D. Vitalini, P. Mineo, *Macromolecules* 1996, **29**, 5520-5528.
- 2 R. G. Little, J. A. Anton, P. A. Loach, J. A. Ibers, *J. Heterocycl. Chem.* 1975, **12**, 343-349.
- 3 P. Mineo, D. Vitalini, E. Scamporrino, *Macromol. Rapid Commun.* 2002, **23**, 681-687.
- 4 V. Villari, P. Mineo, E. Scamporrino, N. Micali, *RSC Advances*, 2012, **2**, 12989.
- 5 P. Mineo, E. Scamporrino, D. Vitalini, R. Alicata, S. Bazzano, *Rapid Comm. Mass Spectrom.* 2005, **19**, 2773-2779.
- 6 V. Villari, N. Micali, *J. Pharm. Sci.* 2008, **97**, 1703-1730.
- 7 S. H. Chen, J. Teixeira, *Phys. Rev. Lett.* 1986, **57**, 2583-2586.
- 8 R. Kuroda, T. Harada, Y. Shindo, *Rev. Sci. Instrum.* 2001, **72**, 3802-3810.
- 9 J. Schellman, H. Jensen, *J. Chem. Rev.* 1987, **87**, 1359-1399.